



Herpes Simplex Virus Ribonucleotide Reductase Subunit Association Inhibitors: the Effect and Conformation of β -Alkylated Aspartic Acid Derivatives

Neil Moss,*[†] Robert Déziel,[†] Jean-Marie Ferland,[†] Sylvie Goulet,[†] Paul-James Jones,[‡]

Scott F. Leonard,[‡] T. Phil Pitner[‡] and Raymond Plante[†]

[†]Bio-Méga/Boehringer Ingelheim Research Inc., 2100 Cunard, Laval, Quebec, Canada, H7S 2G5

[‡]Boehringer Ingelheim Pharmaceuticals Inc., 900 Ridgebury Road, P.O. Box 368, Ridgefield, CT 06877, U.S.A.

Abstract—Incorporating β -alkylated aspartic acid derivatives into herpes simplex virus ribonucleotide reductase subunit association inhibitors can improve inhibitor potency up to 50 times over the corresponding inhibitors containing an unsubstituted aspartic acid. A combination of NMR studies, conformational analysis, and molecular mechanics calculations suggests that the β -alkyl group improves inhibitor potency by favoring the bioactive conformation of the critical aspartic acid carboxyl group. Further support for this hypothesis is provided by a potent conformationally restricted aspartic acid derivative in which the carboxyl group is locked in the putative bioactive conformation.

Introduction

The enzyme ribonucleotide reductase (RR) catalyzes the conversion of ribonucleoside diphosphates into the corresponding deoxy-analogs required for DNA synthesis. RR is composed of two distinct subunits, and peptides corresponding to the C-terminus of the enzyme's smaller subunit (R2) are known to inhibit enzymatic activity by preventing subunit association.¹ Subunit association requires the small subunit C-terminus,² and consequently, peptides that mimic the C-terminus inhibit subunit association by competitively binding to the enzyme's larger subunit (R1). This inhibition is known to be specific for the RRs of herpes viruses, *E. coli*, and mammals.³ Since the small subunit C-termini of these three species have little sequence homology, peptide inhibitors based on these sequences do not cross-inhibit other RRs. These discoveries encouraged us to use the C-terminal amino acid sequence of the herpes simplex virus (HSV) RR small subunit as a lead for the potential development of a new and selective treatment for herpes infections.

In a recent report,⁴ we described a comprehensive structure-activity study based on the 5 C-terminal amino acids of the HSV RR small subunit (H-Val-Val-Asn-Asp-Leu-OH, compound 1). Modification of peptide sequence 1 by (a) replacement of the N-terminal valine by a diethylacetetyl group, (b) addition of a methyl group to the adjacent valine, and (c) replacement of the asparagine NH₂ with pyrrolidine improved inhibitor potency over 1000 times (*c.f.* compounds 1 and 2, Table 1). This report also established the relative contribution of the 5 amino acid side chains to inhibitor potency. These results allowed us to hypothesize how each side chain contributes to inhibitor binding. The aspartic acid carboxyl group in 2 proved to be an essential element for inhibitor potency. Replacement of

the aspartic acid with alanine or glutamic acid lowered activity more than 1500 times. Even replacement with asparagine lowered potency 100 times. Based on these observations, we suggested that the carboxyl group is involved in a relatively precise binding interaction with the large subunit.

Table 1.

Compound	IC ₅₀ (nM) EnzymeAssay
1	760000
2	600
3	180

Our previous report also revealed that replacement of the two aspartic acid β -hydrogens with methyl groups improved inhibitor potency approximately 5 times (*c.f.* compounds 2 and 3). This result motivated us to investigate if further gains in potency could be achieved with different alkyl groups. Considering the importance of the aspartic acid carboxyl group for inhibitor potency, we

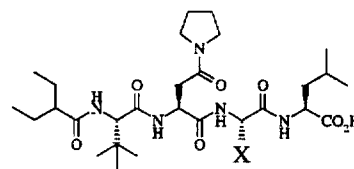
were also interested in explaining the observed potency increase. This report details a series of inhibitors containing β -alkylated and β,β -dialkylated aspartic acid derivatives. A combination of NMR studies, conformational analysis, and molecular mechanics calculations provides a rationale for the observed potencies.

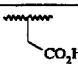
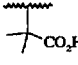
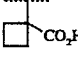
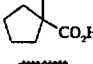
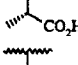
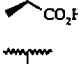
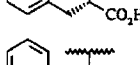
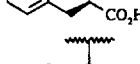

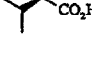
Results and Discussion

Structure-activity studies

Compounds **2** and **3** serve as a point of reference for the series of β -alkylated aspartic acid derivatives shown in Table 2 (see Experimental section for syntheses and stereochemical assignments). A binding assay,⁵ which measures the ability of the inhibitors to compete with a radiolabeled tracer (inhibitor) for binding to immobilized HSV RR large subunit, established the potencies of all inhibitors. This assay is approximately 500 times more sensitive than the conventional enzyme assay and was necessary for the ranking of the more potent inhibitors. The conventional enzyme assay is limited to compounds having IC_{50} s greater than 100 nM.

Table 2.



Compound	X	IC_{50} (nM) Binding Assay
2		336 ± 22
3		43 ± 5
4		9.0 ± 1.7
5		6.4 ± 0.5
6		15 ± 2
7		424 ± 74
8		19 ± 3
9		536 ± 77
10		8.0 ± 1.0
11		845 ± 83

The most effective substitutions found in this study include the cyclobutyl, cyclopentyl, and (*R*)- β -isopropyl-L-aspartic

acid derivatives **4**, **5**, and **10**. These derivatives improve inhibitor potency 30 to 50 times over the corresponding unsubstituted aspartic acid. In related inhibitor series, these beneficial modifications also provide compounds that prevent HSV replication in tissue culture.⁶

The structure-activity study shown in Table 2 reveals three principal findings: (a) cyclopentyl and cyclobutyl aspartic acid derivatives **4** and **5** inhibit 5 to 7 times better than the dimethyl aspartic acid derivative **3**, (b) mono- β -alkylated aspartic acid derivatives also improve activity but the effect is stereochemistry dependent—an (*R*)-alkyl group (compounds **6**, **8**, and **10**) increases activity relative to compound **2** while an (*S*)-alkyl group (compounds **7**, **9**, and **11**) decreases activity slightly, and (c) the size of the monoalkyl group does not affect activity as much as the stereochemistry of the alkyl group. This last observation suggests that the β -alkyl group does not significantly interact with the binding sites on the large subunit. The similar potencies observed for inhibitors having a methyl group and a sterically more demanding benzyl or isopropyl group argue against direct binding involvement. We therefore hypothesized that the β -alkyl group influences inhibitor conformation, especially the conformation of the critical neighboring carboxyl group.

NMR Studies

NMR Studies of the inhibitors in Table 2 revealed that the aspartic acid moieties in compounds **6–11**, in particular, demonstrate preferred solution conformation. The NMR data shown in Table 3 allow a number of conclusions regarding aspartic acid conformation. Firstly, the mono- β -alkylated aspartic acid derivatives in compounds **6–11** appear to have a more defined solution conformation in DMSO than the unsubstituted aspartic acid in compound **2**. The small or large aspartic acid $H\alpha$ - $H\beta$ coupling constants observed for compounds **6–11** (3.5–4 Hz for compounds **6**, **8**, and **10** and 9–10.5 Hz for compounds **7**, **9**, and **11**) support preferred side-chain conformation and contrast with the 5.5 and 6.5 Hz coupling constants observed for compound **2**, values that indicate greater side-chain conformational averaging. The $H\alpha$ - $H\beta$ coupling constants observed for compounds **8–11** in pH 7 buffered D_2O also suggest preferred side-chain conformation. However, the coupling constants observed for the methyl analogs **6** and **7** indicate greater side-chain conformational averaging in D_2O than the corresponding benzyl and isopropyl analogs **8–11**.

A second significant conclusion from the NMR data is that the orientation of the critical aspartic acid carboxyl group depends on the configuration of the β -alkyl group. The relatively large $H\alpha$ - $H\beta$ coupling constants observed for the less potent (*S*)-alkyl compounds **7**, **9**, and **11** support the carboxyl orientation shown in conformation **B1** (Figure 1). However, the small $H\alpha$ - $H\beta$ coupling constants observed for the more potent (*R*)-alkyl compounds **6**, **8**, and **10** support two possible carboxyl orientations (see conformations **A2** and **B2**, Figure 1). This ambiguity can be resolved by an analysis of molecular geometry, employing distances derived from NOE measurements and

angles derived from vicinal coupling constants. Table 4 presents this type of data for the isopropylaspartic acid moiety in compounds **10** and **11**. The distances shown for compound **10** rule out **B2** as the predominant conformation (Figure 2). The 2.8 Å H α -CH₃ distance is inconsistent with conformation **B2**. Taken in context of all the distances measured, the absence of an aspartic acid NH-H β NOE and the very weak or absence of aspartic acid NH-CH₃ NOEs is also inconsistent with conformation **B2**. The approximately 180° H β -H γ dihedral angle (coupling constant 10.5 Hz, Table 3) positions the aspartic acid NH

and a methyl group in **B2** well within 2 Å; this would have produced a very large NOE. The NMR data for compounds **6** and **8** are also consistent with the aspartic acid side-chain conformation **A2**. Complete NOE and vicinal coupling constant data have also been used to provide input for distance geometry calculations on compounds **6–11**. These calculations confirm the aspartic acid side-chain orientation in each case and also provide information on the overall inhibitor conformation. These results will be the subject of a separate publication.

Table 3.

Aspartic Acid Coupling Constants (Hz)

	2	3	4	5	6	7	8	9	10	11
H α -H β DMSO-d ₆	5.5, 6.5	-	-	-	4	9	3.5	9	4	10.5
H α -H β D ₂ O	-	-	-	-	6	8.5	4.5	9.5	3.5	11
H β -H γ DMSO-d ₆	-	-	-	-	7	7	9.5, 5.5	11, 4	10.5	4
H α -NH DMSO-d ₆	8.5	10	10	10	10	9.5	9.5	9.5	9.5	10

Chemical Shifts (ppm) - DMSO-d₆

	2	3	4	5	6	7	8	9	10	11
Aspartic Acid-H α	4.61	4.95	4.90	4.97	4.51	4.67	4.34	4.96	4.52	4.70
Aspartic Acid-H β	-	-	-	-	3.02	2.64	3.30	2.90	2.67	2.53
Aspartic Acid-NH	8.19	8.28	8.18	8.27	7.61	8.36	7.72	8.55	7.62	8.56
Leucine-NH	7.88	7.98	7.96	8.00	8.00	7.90	8.03	7.95	8.00	7.82

Table 4.

NOE		Compound 10		Compound 11	
Atom #1	Atom #2	J-derived dihedral angle and theoretical distance (Å)	NOE-derived distance (Å)	J-derived dihedral angle and theoretical distance (Å)	NOE-derived distance (Å)
Asp NH	Asp H α	180°, d=2.97	†	180°, d=2.97	3.0±0.5 [†]
Asp NH	Asp H β		*		2.8±0.3
Asp NH	Asp H γ		2.8±0.3		2.6±0.3
Asp NH	CH ₃ (1) [‡]		*		*
Asp NH	CH ₃ (2) [‡]		*		4.8±1.0
Asp H α	Asp H β	60°, d=2.42	2.4±0.2 [‡]	180°, d=3.02	3.3±0.5 [‡]
Asp H α	Asp H γ		3.3±0.5		3.3±0.5
Asp H α	CH ₃ (1) [‡]		3.7±0.5		*
Asp H α	CH ₃ (2) [‡]		2.8±0.3		2.4±0.2
Asp H β	Asp H γ	180°, d=3.02	3.3±0.5 [‡]	60°, d=2.42	2.4±0.2 [‡]
Asp H β	CH ₃ (1) [‡]		3.2±0.5		3.0±0.5
Asp H β	CH ₃ (2) [‡]		3.3±0.5		*
Leu NH	Asp NH		3.0±0.5		2.9±0.3
Leu NH	Asp H α		2.9±0.3		2.9±0.3
Leu NH	Asp H β		*		*

[†]A crosspeak was observed, but no distance was determined because of significant overlap with another strong crosspeak.

*Indicates no crosspeak or a very weak, ambiguous crosspeak in ROESY spectrum.

[‡]The names given to the two methyl groups are arbitrary and are not intended to suggest stereochemical identity.

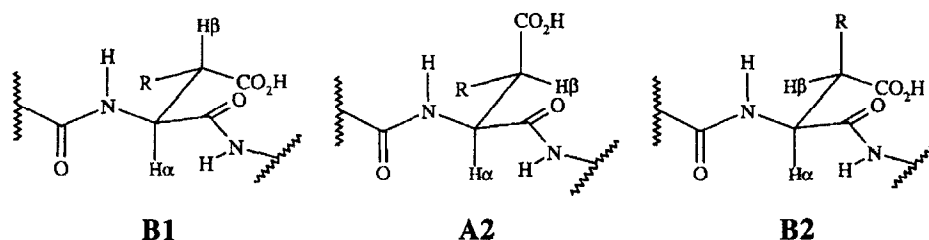


Figure 1. Conformations of β -alkyl aspartic acid derivatives

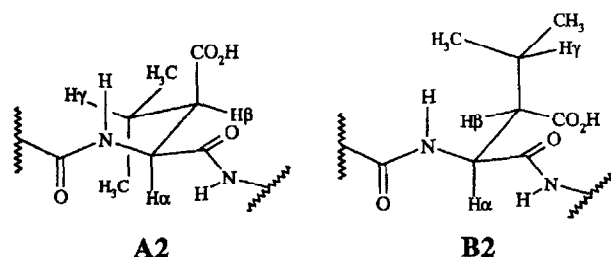


Figure 2. Conformations of (*R*)-isopropylaspartic acid

The superior activity of the (*R*)- β -alkyl compounds **6**, **8**, and **10** over the corresponding (*S*)- β -alkyl compounds **7**, **9**, and **11** correlates with the solution conformation of the critical aspartic acid carboxyl group. Since all the most potent mono- β -alkyl isomers favor conformation **A2** in solution, we hypothesized that this conformation may be similar to the bioactive conformation—that is, the conformation of the aspartic acid moiety upon binding to the large subunit. The corresponding less potent (*S*)- β -alkyl isomers, which favor conformation **B1** in solution, would require a 120° rotation of the aspartic acid $C\alpha$ - $C\beta$ bond in order to bind in the same manner as the corresponding (*R*)-isomer. Energy would be required to produce this conformational change. As a consequence, inhibitory potency would be expected to decrease.

In contrast to the aspartic acid carboxyl, the local aspartic acid backbone conformation in compounds **3–11** appears to be independent of the size or configuration of the β -alkyl group. At the bottom of Table 4 are inter-residue distances involving aspartic acid hydrogens and the leucine NH for compounds **10** and **11**. The invariance of these distances and the invariance of the NH- $H\alpha$ coupling constants (Table 3) indicate that the change in β -chirality has little influence on the local backbone conformation. In fact, consistently large aspartic acid NH- $H\alpha$ coupling constants (dihedral angle approximately 180° , Table 3) are observed for all compounds **3–11**, and distance geometry calculations which include leucine NH to aspartic acid hydrogen NOEs are consistent for all compounds **6–11**. Thus the β -alkyl group seems to influence primarily the conformation of the aspartic acid side chain. As further support for this, we find that relative potency increases associated with the aspartic acid β -alkyl group do not heavily depend on the structure of the adjacent amino acid residues.⁸ These observations suggest that the use of β -alkylated aspartic acid derivatives to favor specific carboxyl group orientations may be applicable to other biologically active peptides.⁹

Conformational analysis

The lack of β -hydrogens in β,β -dialkylated aspartic acid derivatives **3**, **4**, and **5** precludes the use of NMR to determine the carboxyl group orientation in these derivatives. A detailed conformational analysis of the three distinct aspartic acid conformations obtained on rotation about the $C\alpha$ - $C\beta$ bond addresses this question and also provides a rationale for the observed aspartic acid solution conformations.

Analysis of the three staggered aspartic acid side-chain conformations in compounds **2–11** requires ranking the steric environments of the three rotameric positions ($\chi^1 = -60^\circ$, 180° , and 60° , see Figure 3) and ranking the relative steric sizes of alkyl and carboxyl groups. An alkyl group (methyl, benzyl, or isopropyl) is generally considered sterically larger than a carboxyl group.¹⁰ The steric environments of the three rotameric positions can be ranked based on known amino acid side-chain rotameric preferences found in peptides and proteins (see Figure 3). A statistical analysis of χ^1 for aspartic acid and other mono- β -branched amino acids found in proteins¹¹ and peptides¹² found $\chi^1 = -60^\circ$ the most frequently (45–55 %), $\chi^1 = 180^\circ$ the second most frequently (25–30 %), and $\chi^1 = 60^\circ$ the least frequently (15–20 %). The relative preferences for these three conformations can at least be partially explained on the basis of steric interactions between the β -substituent and the three neighboring groups, hydrogen (smallest), NHR (intermediate) and COR' (largest).¹² For $\chi^1 = 60^\circ$, the β -substituent will be *gauche* to the two largest groups (COR' and NHR) so would be predicted to be least favored. For $\chi^1 = -60^\circ$ the β -substituent will be *gauche* to the two smallest groups (hydrogen and NHR) so would be predicted to be most favored.

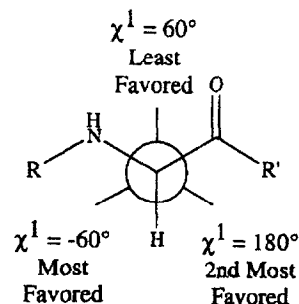


Figure 3.

Figure 4 shows the three staggered conformations resulting from rotation about the $C\alpha$ – $C\beta$ bond for the (*R*)- β -alkyl derivatives 6, 8, and 10, the (*S*)- β -alkyl derivatives 7, 9, and 11, and the β,β -dialkyl derivatives 3–5. A box highlights the predicted favored conformation in each series. Considering the steric factors just discussed, one can readily explain the solution conformation observed for compounds 7, 9, and 11. Conformation B1, which is consistent with the NMR data, should be the preferred conformation as it has the best combination of steric interactions. The bulkier alkyl group occupies the sterically most favored position and the carboxyl group occupies the second most favored position. Based on the same steric considerations, conformations A1 or C1 would be predicted to be higher in energy than B1.

Conformational analysis of the corresponding (*R*)-monoalkyl aspartic acid derivatives 6, 8, and 10 is not quite as straightforward. Conformation A2, which is consistent with the observed NMR data, also positions the bulkier alkyl group in the sterically most favored position. This favorable positioning presumably governs which conformation has the lowest energy. Conformation B2 has the worst possible combination of steric interactions, so it should be higher in energy. However, conformation C2 would be predicted to be relatively close in energy to conformation A2. It may be significant that the isopropyl derivative 10 has the best activity of the three (*R*)- β -substituted aspartic acid derivatives. A bulkier β -isopropyl group should favor conformation A2 more than a sterically smaller methyl or benzyl group.

A similar conformational analysis of the β,β -dialkylated aspartic acid derivatives 3–5 predicts conformation A3 to

predominate. This conformation has the smaller carboxyl group in the sterically least favored position and the two bulkier alkyl groups in the two sterically more favored positions. The other two conformations B3 and C3 would presumably be higher in energy. Thus the predicted conformation of the β,β -dialkylated aspartic acid carboxyl coincides with the conformation observed for the (*R*)- β -monoalkylated derivatives.

A subtle steric effect may explain the increased potencies of cyclobutyl and cyclopentyl aspartic acid derivatives 4 and 5 over the corresponding dimethyl derivative 3. Neighboring hydrogens in 4- and 5-membered rings are not perfectly staggered. When a ring methylene is in the sterically least favored rotameric position, a $C\gamma$ ring hydrogen will be forced to orient closer to the peptide backbone than would the corresponding $C\gamma$ hydrogens of a methyl group. Thus in effect, a ring methylene becomes bulkier than a methyl group. This would raise the energy of conformations B3 and C3 more than conformation A3.

Molecular modeling studies

Molecular mechanics calculations also provide a qualitative prediction of the preferred side-chain conformation for the various β -alkylated aspartic acid derivatives (see Experimental section for minimization procedures). Table 5 lists calculated energy differences (kJ) between the three principal conformations obtained on rotating about the $C\alpha$ – $C\beta$ bond for the aspartic acid derivatives found in compounds 2–11. We simplified the calculations by modeling only *N*-acetylaspartic acid-*N'*-methylamide carboxylate derivatives. The conformations of the two amides in these lowest energy structures are

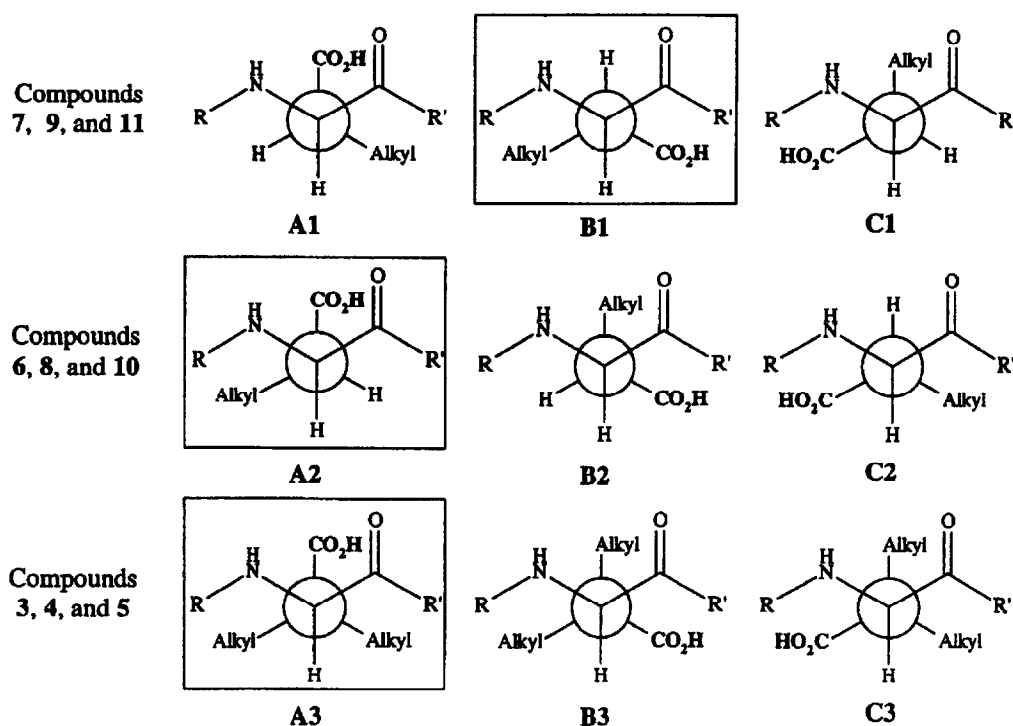


Figure 4.

essentially the same for all three side-chain conformations and are observed irrespective of the β -substitution or its configuration. These amide conformations are also consistent with the NMR coupling constants and NOE data. Although calculated energy differences between the three side-chain conformations are quite small, the calculated lowest energy conformation agrees in each case with the favored conformation suggested by NMR and the conformational analysis study.

Conformational restriction

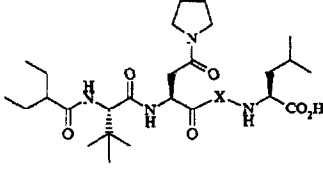
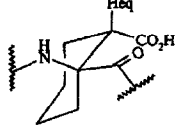
The combination of NMR data, conformational analysis,

and molecular mechanics calculations indicates that the most potent inhibitors favor a χ^1 angle of 60° for the critical aspartic acid carboxyl group. To further test the importance of this conformation for good inhibitor potency, we prepared the conformationally restricted aspartic acid derivative **12** (Table 6). The carboxyl group in this molecule is essentially locked in the postulated bioactive conformation. H_{ax} coupling constants of 12.5 and 4 Hz provide support for this particular chair conformation in solution. Compound **12** is six times more potent than compound **2**. The fact that compound **12** has good inhibitor potency provides strong support for the postulated carboxyl group bioactive conformation.

Table 5.

Corresponding Inhibitor	Differences in calculated conformational energy (kJ)		
	A	B	C
2 R=R'=H	0.08	1.03	0.00
3 R=R'=Methyl	0.00	3.10	4.26
4 R=R'=(CH ₂) ₃	0.00	6.5	7.1
5 R=R'=(CH ₂) ₄	0.00	5.47	6.33
6 R=Methyl R'=H	0.00	6.51	3.47
7 R=H R'=Methyl	2.12	0.00	0.49
8 R=Benzyl R'=H	0.00	7.35	3.58
9 R=H R'=Benzyl	4.74	0.00	1.73
10 R=Isopropyl R'=H	0.00	12.66	6.78
11 R=H R'=Isopropyl	0.78	0.00	1.22

Table 6.

Compound	X	IC ₅₀ (nM) Binding Assay
12		56 ± 8
13		33000 ± 1000

Although compound **12** is more potent than compound **2**, it is not quite as potent as the related acyclic analogues **6**, **8**, and **10**. Steric interactions between the C α ring methylene and the adjacent N-terminal amide may account for this. The approximately 180° dihedral angle between the aspartic acid NH and H α observed for compounds **3–11** would not be as favored in compound **12**.

The synthesis of the rigid aspartic acid derivative in compound **12** also afforded the corresponding C β epimer. We were somewhat surprised to find that this derivative adopts the chair conformation shown in compound **13**. Small H_{eq} coupling constants (3.5, 3.5 Hz) confirm that this chair conformation, which has two axial and one equatorial substituent, predominates in solution. Compound **13** essentially prevents the carboxyl group from adopting the putative bioactive conformation, explaining, at least in part, the 100 times lower activity as compared to compound **2**.

Conclusion

We have shown that alkylating the β -carbon of the aspartic acid residue in herpes simplex virus ribonucleotide reductase subunit association inhibitors can improve inhibitor potency up to 50 times. This improvement in potency is believed to be a consequence of the β -alkyl groups favoring the putative bioactive conformation of the important aspartic acid carboxyl group. In general, it may be possible to control aspartic acid carboxyl conformation in peptides by introducing the appropriate β -alkyl substituent. (*R*)- β -Alkyl groups or β,β -dialkyl groups favor a χ^1 of 60° for the carboxyl group, (*S*)- β -alkyl group favors a χ^1 of 180° , and based on literature observations, no substituent favors a χ^1 of -60° .

Experimental

Ribonucleotide reductase inhibition assays

The effect of our peptide derivatives in an HSV RR binding assay was measured according to published protocol.⁵ The reported IC₅₀ values are the mean of at least three separate determinations and the standard deviation from the mean is also reported.

NMR Studies and distance geometry

¹H NMR experiments conducted on inhibitors 2–13 were performed at 500 MHz with a Bruker AM-500 spectrometer, at 293 K in DMSO-*d*₆ or D₂O buffered to pH 7 with Na₂HPO₄. A standard protocol included conducting a one dimensional experiment and three two dimensional experiments: DQ filtered COSY^{7c} and TOCSY^{7d,e,f} for assignment of proton resonances, and ROESY^{7a,b} (200 msec mix) for assignment of proton resonances and interproton distances. ¹H NMR experiments conducted on intermediates were performed at 400 MHz with a Bruker AMX400 spectrometer.

Distance geometry calculations were performed on a Silicon Graphic 4D-35 Personal Iris computer using DSPACE (Hare Research Inc.). ROESY crosspeak volumes were measured using the volume integration routine in UXNMR (Bruker Instruments Inc.). The distances *r*, obtained using the relation $r = kV^{(-1/6)}$, were converted into distance bounds for distance geometry calculations according to the following schedule: for *r* = 2.0 Å–2.5 Å, the lower bound was obtained by subtracting 0.2 Å from *r* and the upper bound by adding 0.2 Å to *r*; for *r* = 2.5 Å–3.0 Å, ± 0.3 Å; for *r* = 3.0 Å–4.0 Å, ± 0.5 Å; and for *r* > 4.0 Å, ± 1.0 Å. The value of the calibration constant *k* was determined using well-resolved NH–H α crosspeaks, not necessarily from the aspartic acid moiety, for which a coupling constant of 9.5 Hz or greater was observed ($\theta = 180^\circ$, *d* = 2.97 Å). This calibration was checked against the H α –H β and H β –H γ vicinal hydrogen pairs in the isopropyl aspartic acid (among others) in which the distances obtained from the NOE crosspeaks correlate well with the distances derived from the coupling constants. Volumes of ROESY crosspeaks involving the methyl groups were scaled by 1/3 (three hydrogens per methyl) before

conversion to the corresponding distance. Distances involving the methyl groups are referenced to a pseudoatom located at the rotationally-averaged position of the three hydrogen atoms. In calculating the *J*-derived distances reported in Table 4, coupling constants greater than 9.5 Hz were assumed to represent a *trans* orientation ($\theta = 180^\circ$) of the two hydrogen atoms. Coupling constants of 4.0 Hz or lower were assumed to represent a *gauche* orientation ($\theta = 60^\circ$). The reported theoretical distances were derived from an idealized isopropylaspartic acid structure in which the dihedral angle in question was set to the appropriate angle (180° or 60°). This structure was generated and refined using DSPACE using the database of natural amino acid structures to create a model of the isopropylaspartic acid.

Molecular modeling studies

The derivatives in Table 4 were subjected to both systematic (30° rotations of all rotatable bonds) and Monte Carlo (1000 structures) conformational searches using the force field MM2 as implemented in MacroModel v4. Generated structures were minimized by the Polak–Ribier conjugate gradient method (1000 iterations). Both methods of conformational searching found the same energy minima. The carboxylate anion was modeled as opposed to the free acid since the anion better represents the actual species that interacts with the RR large subunit. Energy minimizations were conducted using MM2 default partial charges. A dielectric constant of 80 was used to help dampen long range electrostatic interactions. This adjustment allowed the calculations to better mimic a polar solvent environment. For aspartic acid derivatives calculated without adjusting the dielectric constant to 80 (i.e. default dielectric constant of 1), structures with strong hydrogen bonds between both amide NHs and the carboxyl group dominated the lowest energy conformations. The β -alkyl group did not affect the predominance of these hydrogen bonded structures. These hydrogen bonded structures may be prevalent in the gas phase, but should not be as favored in polar solvent where intermolecular hydrogen bonding with solvent is possible.

Materials

N-Boc-*L*-*tert*-Butyl glycine and leucine-*O*-benzyl ester pTsOH salt were obtained from commercial sources. Boc-2(*S*)-Amino-4-pyrrolidino-4-oxobutanoic acid was prepared according to the procedure in reference 4.

Preparation of β -monoalkyl-*L*-aspartic acid derivatives found in compounds 6–11 (compounds 18 and 19)

See Scheme I. To a solution of KHMDS (0.5 M in toluene, 2 mmol) in dry THF (8 mL) at -78°C was added *N*-Boc-*L*-aspartic acid dibenzyl ester (1 mmol) in dry THF (5 mL + 2 mL rinse). The reaction mixture was stirred at -78°C for 30 min after which time it was treated with either methyl iodide, benzyl bromide, or isopropyl triflate¹³ (1.3 mmol, 2 mmol for isopropyl triflate). The resulting mixture was stirred at -78°C for 30 min, the cooling bath was removed, and after 15 min, acetic acid (3 mmol) was added. This mixture was partitioned between 5 % aqueous citric acid

and ethyl acetate. The organic phase was washed with water and brine, dried (MgSO_4), filtered and concentrated to afford the crude product mixture. Isomers **18** and **19** were isolated pure by flash chromatography. Isomer **18** eluted first in all three cases. See Scheme II for observed isomer ratios and combined yields. Compound **18**, R = methyl: 400 MHz ^1H NMR (CDCl_3) δ 7.36–7.24 (m, 10H), 5.41 (d, $J = 10$ Hz, 1H), 5.09–4.99 (m, 4H), 4.56 (dd, $J = 10, 3.5$ Hz, 1H), 3.31–3.28 (m, 1H), 1.43 (s, 9H), 1.25 (d, $J = 7.5$ Hz, 3H); $[\alpha]_D = -5.9^\circ$ (c 1.31, MeOH). Compound **19**, R = methyl: 400 MHz ^1H NMR (CDCl_3) δ 7.37–7.29 (m, 10H), 5.25 (d, $J = 9$ Hz, 1H), 5.15–5.01 (m, 4H), 4.70 (dd, $J = 9, 4.5$ Hz, 1H), 3.07–3.00 (m, 1H), 1.42 (s, 9H), 1.19 (d, $J = 7.5$ Hz, 3H); $[\alpha]_D = -23.1^\circ$ (c 1.38, MeOH). Compound **18**, R = benzyl: 400 MHz ^1H NMR (CDCl_3) δ 7.31–7.15 (m, 15H), 5.56 (d, $J = 10$ Hz, 1H), 5.08–4.92 (m, 4H), 4.50 (dd, $J = 10, 3.5$ Hz, 1H), 3.45–3.40 (m, 1H), 3.09 (dd, $J = 13.5, 8.5$ Hz, 1H), 2.84 (dd, $J = 13.5, 7.5$ Hz, 1H), 1.45 (s, 9H); $[\alpha]_D = +0.8^\circ$ (c 1.06, MeOH). Compound **19**, R = benzyl: 400 MHz ^1H NMR (CDCl_3) δ 7.34–7.02 (m, 15H), 5.32 (d, $J = 9$ Hz, 1H), 5.13 (d, $J = 12$ Hz, 1H), 5.07 (d, $J = 12$ Hz, 1H), 4.95 (s, 2H), 4.72 (dd, $J = 9, 5$ Hz, 1H), 3.28–3.22 (m, 1H), 3.08 (dd, $J = 13.5, 9.5$ Hz, 1H), 2.80 (dd, $J = 13.5, 5.5$ Hz, 1H), 1.42 (s, 9H); $[\alpha]_D = -15.7^\circ$ (c 3.22, MeOH). Compound **18**, R = isopropyl, mp = 59–60 $^\circ\text{C}$: 400 MHz ^1H NMR (CDCl_3) δ 7.36–7.22 (m, 10H), 5.72 (d, $J = 10$ Hz, 1H), 5.07–4.94 (m, 4H), 4.63 (dd, $J = 10, 4$ Hz, 1H), 2.75 (dd, $J = 9.5, 4$ Hz, 1H), 2.09–2.03 (m, 1H), 1.43 (s, 9H), 0.99 (d, $J = 6.5$ Hz, 3H), 0.91 (d, $J = 6.5$ Hz, 3H); $[\alpha]_D = -9.3^\circ$ (c 1.02, MeOH). Compound **19**, R = isopropyl: 400 MHz ^1H NMR (CDCl_3) δ 7.35–7.29 (m,

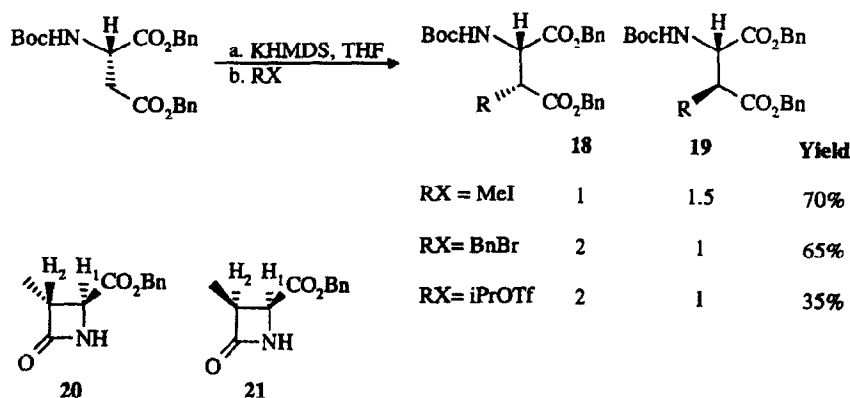
10H), 5.17 (d, $J = 7$ Hz, 1H), 5.14–4.97 (m, 4H), 4.65 (dd, $J = 7, 6$ Hz, 1H), 2.70 (dd, $J = 8.5, 6$ Hz, 1H), 2.20–2.12 (m, 1H), 1.41 (s, 9H), 1.04 (d, $J = 6.5$ Hz, 3H), 0.89 (d, $J = 6.5$ Hz, 3H); $[\alpha]_D = -35^\circ$ (c 2.05, MeOH).

Assignment of relative stereochemistry for β -monoalkyl-L-aspartic acid derivatives **18** and **19**

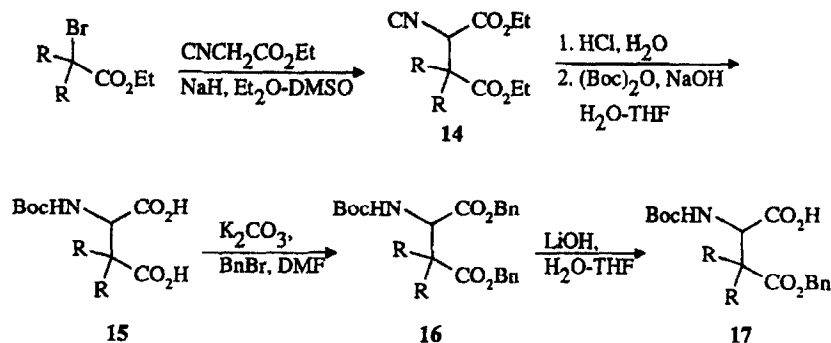
Evidence for the relative stereochemistry assigned in compounds **18** and $\mathbf{19}$ (R = methyl) was obtained upon conversion to their respective β -lactam derivatives **20** and **21** (Scheme I).¹⁴ The H_1 – H_2 coupling constants of 2.5 Hz for compound **20** and 6 Hz for compound **21** are consistent with known β -lactam *cis* and *trans* proton coupling constants. Assignment of the stereochemistry in compounds **18** and **19** when R = benzyl and R = isopropyl was made based on the consistency in NMR data (previous section) and TLC R_f s observed for the three analogs of **18** and **19** respectively.

Preparation of β,β -dialkylaspartic acid derivatives found in compounds **3–5** (compounds **17**)

The preparation of these aspartic acid derivatives was based on a procedure published for β,β -dimethyl-D,L-aspartic acid (see Scheme II).¹⁵ The dimethyl, cyclobutyl and cyclopentyl aspartic acid derivatives **17** used in the preparation of inhibitors **3–5** respectively were incorporated as racemates. The diastereomers obtained on coupling these racemic amino acid derivatives with L-leucine-*O*-benzyl ester were separated by flash chromatography after subsequent coupling with Boc-2(*S*)-



Scheme I.



Scheme II.

amino-4-pyrrolidino-4-oxobutanoic acid. Both diastereomers were elaborated to the corresponding final peptide, and in each case, only one diastereomer proved to have inhibitory activity greater than 1000 μ M. The configuration of the dialkylaspartic acid in the active diastereomer was assigned as L based on precedent with other active inhibitors containing L-aspartic acid derivatives (e.g. compounds 6–11) and the fact that a related inhibitor series containing D-aspartic acid did not have inhibitory activity up to 1000 μ M.

The following procedure, which details the preparation of the cyclopentylaspartic acid derivative of 17, was also used for the preparation of the dimethyl and cyclobutyl analogs. To a solution of ethyl-1-bromocyclopentane carboxylate¹⁶ (17.1 g, 77.3 mmol) and freshly distilled ethyl isocyanoacetate (12.7 g, 112 mmol) in a mixture of dry ether (60 mL) and dry DMSO (60 mL) under nitrogen was added NaH (4.5 g, 60 % oil suspension) over a period of 5 h. The resulting red slurry was stirred at room temperature for 16 h. Extra DMSO can be added if stirring becomes difficult. The reaction mixture was treated with saturated aqueous ammonium chloride (5 mL) and then water (500 mL). The mixture was extracted with ethyl acetate (2 \times 200 mL) and the combined organic phases were washed with water (2 \times) and brine, dried (MgSO₄), filtered, and concentrated to afford a dark red oil. Purification by flash chromatography (silica, ethyl acetate:hexane, 1:10) afforded isonitrile derivative 14 as a clear colorless liquid (13 g, 66 %). 400 MHz ¹H NMR (CDCl₃) δ 4.80 (s, 1H), 4.28–4.15 (m, 4H), 2.31–2.26 (m, 1H), 2.07–2.01 (m, 2H), 1.80–1.68 (m, 5H), 1.30 (t, *J* = 7 Hz, 3H), 1.27 (t, *J* = 7 Hz, 3H).

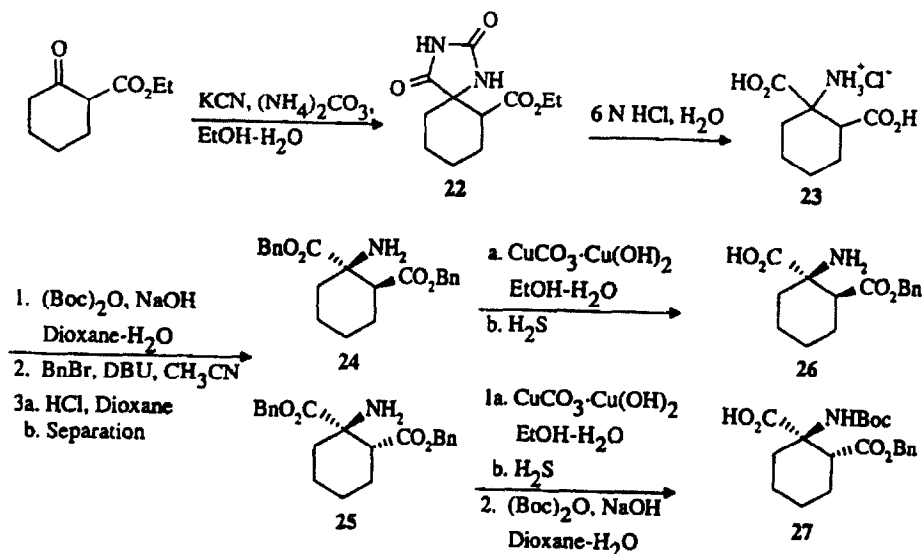
Compound 14 was mixed with 6 N HCl (60 mL) at 0 °C. After dissolution, the reaction mixture was refluxed for 24 h. The solvent was removed and the resulting off white solid was dried under vacuum. The amino acid salt was dissolved in a mixture of dioxane (50 mL) and 3 N aqueous NaOH (53 mL). A solution of di-*tert*-butyl dicarbonate (14.6 g, 67 mmol) in dioxane (20 mL) was added and the reaction mixture was stirred at room temperature for 16 h. The pH of the reaction mixture was maintained at 10–11 by addition of extra 3 N aqueous NaOH if necessary. The reaction mixture was diluted with water (500 mL) and washed with ether (2 \times 300 mL). The aqueous phase was acidified with solid citric acid and extracted with ethyl acetate (2 \times 300 mL). The combined ethyl acetate extracts were washed with water (2 \times) and brine, dried (MgSO₄), filtered and concentrated to afford the *N*-Boc amino acid derivative 15 as a clear viscous gum (14 g, 96 %). To a solution of 15 (7.2 g, 25 mmol) in dry DMF (50 mL) was added potassium carbonate (7.6 g, 55 mmol) and benzyl bromide (6.6 mL, 55 mmol). The reaction mixture was stirred at room temperature for 16 h after which time it was poured into a mixture of water (350 mL) and ethyl acetate (350 mL). The organic phase was washed with water and brine, dried, filtered and concentrated to provide a pale yellow viscous liquid. Purification by flash chromatography provided compound 16 as a white solid (11 g, 94 %) mp 54–55 °C. 400 MHz ¹H NMR (CDCl₃) 7.36–7.25 (m, 10H), 5.54 (d, *J* = 10 Hz,

1H), 5.04 (s, 2H), 5.03 (d, *J* = 12 Hz, 1H), 4.94 (d, *J* = 12 Hz, 1H), 4.53 (d, *J* = 10 Hz, 1H), 2.25–2.20 (m, 1H), 2.10–1.97 (m, 1H), 1.85–1.56 (m, 6H), 1.42 (s, 9H).

To a solution of dibenzyl ester 16 (11 g, 24 mmol) in a mixture of THF (200 mL) and water (50 mL) was added a solution of 1 N aqueous LiOH (25 mL, 25 mmol) over 3 h at a rate that maintained reaction homogeneity. After an additional 3 h at room temperature, the reaction mixture was concentrated to remove the THF, the residue was diluted with water (150 mL), and the aqueous solution was gently washed with ether (3 \times 100 mL). The aqueous phase was acidified with solid citric acid and extracted with ethyl acetate (2 \times). The combined ethyl acetate layers were washed with brine, dried (MgSO₄), filtered and concentrated to afford the monobenzyl ester derivative 17 as a clear gum (7.3 g, 82 %). This material was used in the subsequent coupling reaction with L-leucine-*O*-benzyl ester without further purification. This procedure was also used for the selective α -ester hydrolysis of compounds 18 and 19 (Scheme I).

Preparation of rigid aspartic acid derivatives found in inhibitors 12 and 13 (compounds 26 and 27)

See Scheme III. To a solution of ethyl-2-oxocyclohexanecarboxylate (9.5 g, 56 mmol) in 50 % aqueous ethanol (120 mL) was added KCN (4.4 g, 67 mmol) and ammonium carbonate (17.8 g, 185 mmol). The mixture was stirred at 50 °C for 7 h and then poured into ethyl acetate (250 mL) and water (200 mL). The organic phase was washed with water and brine, dried (MgSO₄), filtered and concentrated to afford the hydantoin mixture 22 as a white solid (8.8 g, 65 %). This material (5.2 g, 22 mmol) was refluxed in 6 N HCl (200 mL) for 7 days. The reaction mixture was washed with ethyl acetate and the aqueous phase was concentrated to provide amino acid mixture 23 as a white solid (5 g). NMR (D₂O) showed a 3.5:1 mixture of isomers.¹⁶ Mixture 23 was converted to the corresponding *N*-Boc derivatives by using the same procedure used for the preparation of compound 15. However it proved very difficult to convert the major isomer (stereochemistry analogous to compound 24) into the corresponding *N*-Boc derivative. The Boc product was obtained as a 1:1 mixture of isomers (30 % yield). A solution of this material (2.3 g, 8 mmol) in dry acetonitrile (20 mL) was treated with DBU (2.4 mL, 16 mmol) and benzyl bromide (2.1 mL, 17 mmol). After 6 h at room temperature, the reaction mixture was poured into ethyl acetate:water and the organic phase was washed with water and brine. Drying (MgSO₄), filtration, concentration, and purification by flash chromatography (silica, hexane:ethyl acetate, 7:1) provided the corresponding dibenzylester mixture as a clear colorless liquid (3.1 g, 87 %). This material was treated with 4 N HCl in dioxane (20 mL) for 30 min. The solvent was removed under vacuum and the residue was partitioned between ethyl acetate and saturated aqueous NaHCO₃. The organic phase was washed with brine, dried (MgSO₄), filtered and concentrated to afford a 1:1 mixture of compounds 24 and 25 (2.2 g, 95 %). These two isomers could be readily separated at this stage by flash chromatography (silica, hexane:ethyl acetate, 1:1).



Scheme III.

Compound **24**, viscous liquid: 400 MHz ^1H NMR (CDCl_3) δ 7.35–7.23 (m, 10H), 5.07–4.98 (m, 4H), 3.04 (dd, $J = 12.5$, 5 Hz, 1H), 2.35 (br s, 2H), 1.98–1.27 (m, 8H). Compound **25**, viscous liquid: 400 MHz ^1H NMR (CDCl_3) δ 7.35–7.27 (m, 10H), 5.12–5.03 (m, 4H), 3.25 (br s, 2H), 2.70 (dd, $J = 11$, 5 Hz, 1H), 2.25–1.29 (m, 8H). A solution of the dibenzyl ester **24** or **25** (0.63 g, 1.7 mmol) in a mixture of ethanol (12 mL) and water (35 mL) was treated with $\text{CuCO}_3\text{-Cu(OH)}_2$ (1.9 g, 8.6 mmol). The resultant heterogeneous mixture was stirred at 70°C for 3 days, after which time H_2S was bubbled through the solution for 15 min. The resultant black mixture was filtered through celite, rinsing with water:ethanol 2:1 and then methanol. Concentration under vacuum afforded the corresponding amino acid derivatives as white solids (0.40–0.47 g, 80–99 %). Product **26** could be coupled directly with leucine-*O*-benzyl ester since the amine function in **26** proved to be very unreactive. The product resulting from the selective debenzoylation of **25** had to be converted to its *N*-Boc derivative **27** before coupling to leucine-*O*-benzyl ester.

Assignment of relative stereochemistry for rigid aspartic acid derivatives found in inhibitors 12 and 13 (compounds 26 and 27)

The Bucherer–Bergs reaction of 2-methyl and 2-phenylcyclohexanone has previously been shown to favor formation of the isomer having the stereochemistry analogous to compound **24**.¹⁷ Confirmation of the relative stereochemistry shown in the rigid aspartic acid derivatives in compounds **12** and **13** was provided by NMR. For compound **13** (see structure in Table 6), H_{eq} has coupling constants of 3.5 and 3.5 Hz and an NOE to the NH shown (Asp NH). For compound **12**, H_{ax} has coupling constants of 12.5 and 4 Hz and no observable NOE to the NH (H_{ax} only shows NOEs to other cyclohexane ring hydrogens). Taken together, this combination of coupling constant and NOE data provide good evidence for the relative stereochemistry present in compounds **12** and **13** as well as the favored chair conformation. This NMR data would not be consistent with either of the rigid aspartic acid

derivatives in compounds **12** or **13** existing in solution with the opposite chair conformation.

The rigid aspartic acid derivatives **26** and **27** used in the preparation of inhibitors **12** and **13** respectively were incorporated as racemates. The diastereomers obtained on coupling these racemic amino acid derivatives with L-leucine-*O*-benzyl ester were separated and elaborated to the final peptide in the same manner as was done for the dialkylaspartic acid derivatives **17**. In each case, only one diastereomer proved to have inhibitory activity greater than $1000 \mu\text{M}$. As was done for inhibitors **3–5**, the active isomer was assigned the corresponding L-configuration.

Inhibitor synthesis

All inhibitors were prepared by solution phase peptide synthesis, in which *N*-Boc-amino acid derivatives were coupled sequentially from C- to N-terminus by using benzotriazol-1-yl-1,1,3,3-tetramethyluronium tetrafluoroborate (TBTU) as the coupling agent and subsequent removal of the *N*-Boc protective group was effected with 4 N HCl in dioxane. The N-terminal diethylacetyl group was also incorporated by using TBTU as the coupling agent. The following procedure is representative. To a solution of *N*-Boc-amino acid (1 mmol) in dry acetonitrile (2.5 mL) was added TBTU (1 mmol) and *N*-methylmorpholine (1 mmol). After approximately 5 min, this solution was added to a solution of amino acid or peptide hydrochloride salt (1 mmol) in dry acetonitrile (2.5 mL) containing *N*-methylmorpholine (2 mmol). The reaction mixture was stirred at ambient temperature for 2 to 6 h (reaction monitored by TLC) and then poured into a mixture of ethyl acetate (50 mL) and saturated aqueous sodium bicarbonate (50 mL). The organic phase was washed with another portion of sodium bicarbonate, 1 N aqueous HCl ($2 \times 50 \text{ mL}$) and brine (50 mL). Drying (MgSO_4), filtration and concentration provided the peptide, usually of sufficient purity to continue to the next step without further purification. *N*-Boc peptide derivatives could be purified if necessary by conventional flash chromatography. The *N*-

Boc-peptide product (1 mmol) was then treated with 4 N HCl in dioxane (5 mL) for 30 min. The solvent was removed under vacuum and the resulting hydrochloride salt was subjected to high vacuum before its use in the next coupling reaction.

Subsequently, the fully protected peptide derivatives were purified by flash chromatography and the two benzylester protective groups were removed by catalytic hydrogenolysis by using 10 % Pd/C (10 mol %) in methanol and 1 atm H₂ for 3 h. The resultant inhibitor was usually obtained in greater than 95 % purity (HPLC and NMR), but if necessary it could be purified by preparative HPLC on a C18 reverse-phase column (Vydac, 15 μ m particle size) eluting with 0.06 % aqueous TFA–0.06 % TFA in acetonitrile gradients.

Inhibitor characterization and purity

NMR Spectra were recorded on a Bruker AM-500 (500 MHz for ¹H NMR) spectrometer and were referenced to TMS as an internal standard (0 ppm δ scale). Data are reported as follows: chemical shift (ppm), multiplicity (s = singlet, d = doublet, t = triplet, q = quartet, br = broad), coupling constant (Hertz, reported to the nearest 0.5 Hz), and integration. FAB Mass spectra were obtained from an MF 50 TATC instrument operating at 6 kV and 1 mA by using thioglycerol as a matrix support. Amino acid analyses were performed using vapor phase hydrolysis (6 N HCl containing 0.1 % phenol, 110 °C oven, *in vacuo*) followed by pre-column derivatization with PITC. The resulting PTC amino acids were analyzed/separated on a C18 reverse phase Waters Pico-Tag column. All compounds showed correct amino acid composition, and the reported peptide recoveries were calculated from this amino acid analysis (value \pm 5 % from two separate determinations). Inhibitor HPLC purity was measured by using an analytical C18 reverse phase column and two different eluting systems: method a, 0.06 % TFA in water–0.06 % TFA in acetonitrile gradient (20–100 % acetonitrile over 30 min) and method b, 20 mM aqueous Na₂HPO₄ (pH 7.4)–acetonitrile gradient (20–75 % acetonitrile over 25 min).

Compound 4. ¹H NMR (DMSO-*d*₆) δ 8.37 (d, *J* = 7 Hz, 1H), 8.18 (d, *J* = 10 Hz, 1H), 7.96 (d, *J* = 7.5 Hz, 1H), 7.67 (d, *J* = 9.5 Hz, 1H), 4.90 (d, *J* = 10 Hz, 1H), 4.68 (ddd, *J* = 10.5, 7, 4.5 Hz, 1H), 4.35 (d, *J* = 9.5 Hz, 1H), 4.12 (ddd, *J* = 10.5, 7.5, 4.5 Hz, 1H), 3.43–3.20 (m, 4H), 2.82 (dd, *J* = 16.5, 10.5 Hz, 1H), 2.61 (dd, *J* = 16.5, 4.5 Hz, 1H), 2.30–1.73 (m, 13H), 1.49–1.24 (m, 5H), 0.88 (s, 9H), 0.88 (d, 3H, overlap with singlet), 0.81–0.75 (m, 9H); FAB-MS 666 (M⁺ + H), 688 (M⁺ + Na); A.A.A. 99 % pept. rec.; HPLC method a: 99 %.

Compound 5. ¹H NMR (DMSO-*d*₆) δ 8.37 (d, *J* = 7.5 Hz, 1H), 8.27 (d, *J* = 10 Hz, 1H), 8.00 (d, *J* = 7.5 Hz, 1H), 7.65 (d, *J* = 9.5 Hz, 1H), 4.97 (d, *J* = 10 Hz, 1H), 4.69 (ddd, *J* = 11, 7.5, 4 Hz, 1H), 4.36 (d, *J* = 9.5 Hz, 1H), 4.14 (ddd, *J* = 11.5, 7.5, 4.5 Hz, 1H), 3.41–3.18 (m, 4H), 2.80 (dd, *J* = 16.5, 11 Hz, 1H), 2.57 (dd, *J* = 16.5, 4 Hz, 1H), 2.31–2.25 (m, 1H), 2.04–1.98 (m, 1H), 1.91–1.60 (m, 8H), 1.52–1.26 (m, 10H), 0.88 (s, 9H), 0.88 (d, 3H, overlap with singlet),

0.81–0.75 (m, 9H); FAB-MS 680 (M⁺ + H), 702 (M⁺ + Na); A.A.A. 92 % pept. rec.; HPLC method a: 97 %; method b: 89 %.

Compound 6. ¹H NMR (DMSO-*d*₆) δ 8.37 (d, *J* = 7 Hz, 1H), 8.0 (d, *J* = 8 Hz, 1H), 7.70 (d, *J* = 9.5 Hz, 1H), 7.61 (d, *J* = 10 Hz, 1H), 4.56 (ddd, *J* = 10, 7, 4.5 Hz, 1H), 4.51 (dd, *J* = 10, 4 Hz, 1H), 4.33 (d, *J* = 9.5 Hz, 1H), 4.17 (ddd, *J* = 11, 8, 4.5 Hz, 1H), 3.45–3.33 (m, 2H), 3.25 (t, *J* = 7 Hz, 2H), 3.02 (dq, *J* = 7.5, 4 Hz, 1H), 2.81 (dd, *J* = 16.5, 10 Hz, 1H), 2.62 (dd, *J* = 16.5, 4.5 Hz, 1H), 2.29–2.23 (m, 1H), 1.91–1.73 (m, 6H), 1.51–1.26 (m, 5H), 1.08 (d, *J* = 7.5 Hz, 3H), 0.89 (d, *J* = 6.5 Hz, 3H), 0.88 (s, 9H), 0.81 (d, *J* = 6.5 Hz, 3H), 0.78 (d, *J* = 7.5 Hz, 3H), 0.75 (d, *J* = 7.5 Hz, 3H); FAB-MS 640 (M⁺ + H), 662 (M⁺ + Na); A.A.A. 90 % pept. rec.; HPLC method a: 98 %; method b: 99 %.

Compound 7. ¹H NMR (DMSO-*d*₆) δ 8.36 (d, *J* = 9.5 Hz, 1H), 8.27 (d, *J* = 7.5 Hz, 1H), 7.90 (d, *J* = 7.5 Hz, 1H), 7.66 (d, *J* = 9.5 Hz, 1H), 4.67 (dd, *J* = 9.5, 9 Hz, 1H), 4.58 (ddd, *J* = 9, 7.5, 5 Hz, 1H), 4.29 (d, *J* = 9.5 Hz, 1H), 4.15 (ddd, *J* = 10.5, 7.5, 5 Hz, 1H), 3.41–3.32 (m, 2H) overlap with H₂O, 3.27–3.22 (m, 2H), 2.76 (dd, *J* = 16.5, 9 Hz, 1H), 2.64 (dq, *J* = 9, 7 Hz, 1H), 2.59 (dd, *J* = 16.5, 5 Hz, 1H), 2.30–2.24 (m, 1H), 1.90–1.85 (m, 2H), 1.79–1.72 (m, 4H), 1.49–1.27 (m, 5H), 0.97 (d, *J* = 7 Hz, 3H), 0.89 (s, 9H), 0.88 (d, *J* = 6.5 Hz, 3H), 0.82 (d, *J* = 6.5 Hz, 3H), 0.78 (t, *J* = 7.5 Hz, 3H), 0.75 (t, *J* = 7.5 Hz, 3H); FAB-MS 640 (M⁺ + H), 662 (M⁺ + Na); A.A.A. 110 % pept. rec.; HPLC method a: 95 %; method b: 97 %.

Compound 8. ¹H NMR (DMSO-*d*₆) δ 8.49 (d, *J* = 7 Hz, 1H), 8.03 (d, *J* = 8 Hz, 1H), 7.75 (d, *J* = 9.5 Hz, 1H), 7.72 (d, *J* = 9.5 Hz, 1H), 7.27–7.18 (m, 5H), 4.58 (ddd, *J* = 10, 7, 4.5 Hz, 1H), 4.39 (d, *J* = 9.5 Hz, 1H), 4.34 (dd, *J* = 9.5, 3.5 Hz, 1H), 4.15 (ddd, *J* = 11, 8, 4.5 Hz, 1H), 3.46–3.21 (m, 5H) overlap with H₂O, 2.93 (dd, *J* = 13.5, 5.5 Hz, 1H), 2.86 (dd, *J* = 16.5, 10 Hz, 1H), 2.71 (dd, *J* = 13.5, 9.5 Hz, 1H), 2.66 (dd, *J* = 16.5, 4.5 Hz, 1H), 2.30–2.25 (m, 1H), 1.92–1.73 (m, 6H), 1.48–1.27 (m, 5H), 0.90 (s, 9H), 0.88 (d, *J* = 6.5 Hz, 3H), 0.80 (d, *J* = 6.5 Hz, 3H), 0.78 (t, *J* = 7.5 Hz, 3H), 0.76 (t, *J* = 7.5 Hz, 3H); FAB-MS 738 (M⁺ + H), 760 (M⁺ + Na); A.A.A. 89 % pept. rec.; HPLC method a: 97 %; method b: 99 %.

Compound 9. ¹H NMR (DMSO-*d*₆) δ 8.55 (d, *J* = 9.5 Hz, 1H), 8.33 (d, *J* = 7.5 Hz, 1H), 7.95 (d, *J* = 7.5 Hz, 1H), 7.64 (d, *J* = 9.5 Hz, 1H), 7.24–7.10 (m, 5H), 4.96 (dd, *J* = 9.5, 9 Hz, 1H), 4.63 (ddd, *J* = 9, 7.5, 5 Hz, 1H), 4.30 (d, *J* = 9.3 Hz, 1H), 4.16 (ddd, *J* = 10.5, 7.5, 4.5 Hz, 1H), 3.43–3.33 (m, 2H) overlap with H₂O, 3.25 (t, *J* = 7 Hz, 2H), 2.93–2.86 (m, 2H), 2.91 (dd, *J* = 14, 4 Hz, 1H), 2.78 (dd, *J* = 16.5, 9 Hz, 1H), 2.60 (dd, *J* = 16.5, 5 Hz, 1H), 2.55 (dd, *J* = 14, 11 Hz, 1H) partial overlap with DMSO, 2.28–2.23 (m, 1H), 1.91–1.73 (m, 6H), 1.51–1.24 (m, 5H), 0.89 (d, *J* = 6.5 Hz, 3H), 0.85 (s, 9H), 0.83 (d, *J* = 6.5 Hz, 3H), 0.76 (t, *J* = 7.5 Hz, 3H), 0.74 (t, *J* = 7.5 Hz, 3H); FAB-MS 738 (M⁺ + H), 760 (M⁺ + Na); A.A.A. 101 % pept. rec.; HPLC method a: 97 %; method b: 95 %.

Compound 10. ¹H NMR (DMSO-*d*₆) δ 8.50 (d, *J* = 6.5 Hz, 1H), 8.00 (d, *J* = 8 Hz, 1H), 7.75 (d, *J* = 9.5 Hz, 1H), 7.62

(d, $J = 9.5$ Hz, 1H), 4.52 (dd, $J = 9.5$, 4 Hz, 1H), 4.49 (ddd, $J = 10.5$, 6.5, 4.5 Hz, 1H), 4.34 (d, $J = 9.5$ Hz, 1H), 4.14 (ddd, $J = 11.5$, 8, 4.5 Hz, 1H), 3.46–3.34 (m, 2H), 3.24 (t, $J = 7$ Hz, 2H), 2.89 (dd, $J = 16.5$, 10.5 Hz, 1H), 2.67 (dd, $J = 10.5$, 4 Hz, 1H), 2.59 (dd, $J = 16.5$, 4.5 Hz, 1H), 2.31–2.25 (m, 1H), 1.91–1.65 (m, 7H), 1.51–1.26 (m, 5H), 0.89–0.87 (overlapping d, 6H), 0.87 (s, 9H), 0.82 (d, $J = 6.5$ Hz, 3H), 0.79 (d, $J = 6.5$ Hz, 3H), 0.78 (t, $J = 7.5$ Hz, 3H), 0.75 (t, $J = 7.5$ Hz, 3H); FAB-MS 668 ($M^+ + H$), 690 ($M^+ + Na$); A.A.A. 84 % pept. rec.; HPLC method a: 98 %; method b: 98 %.

Compound 11. 1H NMR (DMSO- d_6) δ 8.56 (d, $J = 10$ Hz, 1H), 8.38 (d, $J = 8$ Hz, 1H), 7.82 (d, $J = 8$ Hz, 1H), 7.70 (d, $J = 9.5$ Hz, 1H), 4.70 (dd, $J = 10.5$, 10 Hz, 1H), 4.56 (ddd, $J = 9$, 8, 5 Hz, 1H), 4.32 (d, $J = 9.5$ Hz, 1H), 4.16 (ddd, $J = 10$, 8, 5 Hz, 1H), 3.41–3.22 (m, 4H), 2.78 (dd, $J = 16.5$, 9 Hz, 1H), 2.56–2.50 (m, 2H), 2.30–2.25 (m, 1H), 1.97 (dh, $J = 7$, 4 Hz, 1H), 1.91–1.85 (m, 2H), 1.80–1.73 (m, 4H), 1.47–1.23 (m, 5H), 0.90 (s, 9H), 0.88–0.86 (overlapping d, 6H), 0.82 (d, $J = 6.5$ Hz, 3H), 0.79 (t, $J = 7.5$ Hz, 3H), 0.76 (t, $J = 7.5$ Hz, 3H), 0.70 (t, $J = 7$ Hz, 3H); FAB-MS 668 ($M^+ + H$), 690 ($M^+ + Na$); A.A.A. 106 % pept. rec.; HPLC method a: 98 %; method b: 98 %.

Compound 12. 1H NMR (DMSO- d_6) δ 8.56 (d, $J = 7$ Hz, 1H), 7.98 (d, $J = 8$ Hz, 1H), 7.78 (d, $J = 9.5$ Hz, 1H), 7.71 (s, 1H), 4.45 (ddd, $J = 11$, 7.5, 4 Hz, 1H), 4.36 (d, $J = 9.5$ Hz, 1H), 4.19 (ddd, $J = 11$, 8, 4.5 Hz, 1H), 3.47–3.43 (m, 1H), 3.37–3.33 (m, 1H), 3.25 (t, $J = 7$ Hz, 2H), 2.95–2.90 (m, 2H), 2.75 (dd, $J = 12.5$, 4 Hz, 1H), 2.49 (dd, $J = 16$, 4 Hz, 1H) overlap with DMSO, 2.30–2.25 (m, 1H), 1.93–1.68 (m, 8H), 1.56–1.25 (m, 11H), 0.90 (s, 9H), 0.87 (d, $J = 6.5$ Hz, 3H), 0.80–0.74 (m, 9H); FAB-MS 702 ($M^+ + Na$); HPLC method a: 98 %; method b: 99 %.

Compound 13. 1H NMR (DMSO- d_6) δ 8.30 (d, $J = 7.5$ Hz, 1H), 7.75 (d, $J = 9$ Hz, 1H), 7.71 (s, 1H), 7.50 (d, $J = 8$ Hz, 1H), 4.60 (ddd, $J = 7.5$, 6.5, 6 Hz, 1H), 4.30 (d, $J = 9$ Hz, 1H), 4.16 (ddd, $J = 10$, 8, 5 Hz, 1H), 3.38–3.27 (m, 4H), 3.03–3.00 (dd, $J = 3.5$, 3.5 Hz, 1H), 2.64–2.60 (m, 2H), 2.37–2.32 (m, 1H), 2.30–2.25 (m, 1H), 1.97–1.92 (m, 1H), 1.89–1.85 (m, 2H), 1.78–1.74 (m, 2H), 1.73–1.24 (m, 13H), 0.92 (s, 9H), 0.83 (d, $J = 6.5$ Hz, 3H), 0.80 (d, $J = 6.5$ Hz, 3H), 0.79 (t, $J = 7.5$ Hz, 3H), 0.75 (t, $J = 7.5$ Hz, 3H); FAB-MS 702 ($M^+ + Na$); HPLC method a: 95 %.

Acknowledgments

We thank R. Krogsrud and E. Welchner for determining the potencies of our inhibitors in the HSV RR binding assay. We are also grateful to Professor D. Liotta, W. Cui, and M. Cardozo for helpful discussions.

References and Notes

- (a) Dutia, B. M.; Frame, M. C.; Subak-Sharpe, J. H.; Clarke, W. N.; Marsden, H. S. *Nature* **1986**, *321*, 439; (b) Cohen, E. A.; Gaudreau, P.; Brazeau, P.; Langelier, Y. *Nature* **1986**, *321*, 441; (c) Gaudreau, P.; Paradis, H.; Langelier, Y.; Brazeau, P. *J. Med. Chem.* **1990**, *33*, 723; (d) Gaudreau, P.; Brazeau, P.; Richer, M.; Cormier, J.; Langlois, D.; Langelier, Y. *J. Med. Chem.* **1992**, *35*, 346; (e) Chang, L. L.; Hannah, J.; Ashton, W. T.; Rasmussen, G. H.; Ikeler, T. J.; Patel, G. F.; Garsky, V.; Uncapher, C.; Yamanaka, G.; McClements, W. L.; Tolman, R. L. *BioMed. Chem. Lett.* **1992**, *2*, 1207.
- Filatov, D.; Ingemarson, R.; Graslund, A.; Thelander, L. *J. Biol. Chem.* **1992**, *267*, 15816.
- Cosentino, G.; Lavallée, P.; Rakhit, S.; Plante, R.; Gaudette, Y.; Lawetz, C.; Whitehead, P. W.; Duceppe, J.-S.; Lépine-Frenette, C.; Dansereau, N.; Guilbault, C.; Langelier, Y.; Gaudreau, P.; Thelander, L.; Guindon, Y. *Biochem. Cell Biol.* **1991**, *69*, 79.
- Moss, N.; Déziel, R.; Adams, J.; Aubry, N.; Bailey, M.; Baillet, M.; Beaulieu, P.; DiMaio, J.; Duceppe, J.-S.; Ferland, J.-M.; Gauthier, J.; Ghiro, E.; Goulet, S.; Grenier, L.; Lavallée, P.; Lépine-Frenette, C.; Plante, R.; Rakhit, S.; Soucy, F.; Wernic, D.; Guindon, Y. *J. Med. Chem.* **1993**, *36*, 3005.
- Krogsrud, R. L.; Welchner, E.; Scouten, E.; Liuzzi, M. *Anal. Biochem.* **1993**, *213*, 386.
- For a preliminary account of this work see Moss, N.; Déziel, R.; Beaulieu, P.; Bonneau, A.-M.; Krogsrud, R. L.; Liuzzi, M.; Plante, R.; Guindon, Y. *Peptides: Chemistry and Biology. Proceedings of the Thirteenth American Peptide Symposium*, pp. 580–582, Hodges, R. S.; Smith, J. A., Eds; Escom; Leiden, 1993.
- (a) Bax, A.; Davis, D. G. *J. Magn. Reson.* **1984**, *63*, 207; (b) Bothner-By, A. A.; Stephens, R. L.; Lee, J.; Warren, C. D.; Jeanloz, R. W. *J. Am. Chem. Soc.* **1984**, *106*, 811; (c) Piantini, U.; Sorensen, O. W.; Ernst, R. R. *J. Am. Chem. Soc.* **1982**, *104*, 6800; (d) Braunshweiler, L.; Ernst, R. R. *J. Magn. Reson.* **1983**, *53*, 521; (e) Davis, D. G.; Bax, A. *J. Am. Chem. Soc.* **1985**, *107*, 2820; (f) Bax, A.; Davis, D. G. *J. Magn. Reson.* **1985**, *65*, 355.
- Manuscripts in preparation will further illustrate this point.
- The conformational properties of β -methylphenylalanine in a bioactive octapeptide have recently been detailed. Kövér, K. E.; Jiao, D.; Fang, S.; Hruby, V. J. *J. Org. Chem.* **1994**, *59*, 991.
- March, J. *Advanced Organic Chemistry*, 4th Ed., p. 145, John Wiley & Sons; New York, 1992.
- (a) Eisenhaber, F.; Argos, P. *J. Mol. Biol.* **1993**, *233*, 592; (b) Bhat, T. N.; Sasisekaran, V.; Vijayan, M. *Int. J. Peptide Protein Res.* **1979**, *13*, 170.
- Benedetti, E.; Morelli, G.; Némethy, G.; Scheraga, H. A. *Int. J. Peptide Protein Res.* **1983**, *22*, 1.
- Wolf, J.-P.; Rapoport, H. *J. Org. Chem.* **1989**, *54*, 3164.
- Baldwin, J. E.; Adlington, R. M.; Gollins, D. W.; Schofield, C. J. *Tetrahedron* **1990**, *46*, 4733.
- Bochenska, M.; Biernat, J. F. *Roczniki Chem.* **1976**, *50*, 1195.
- Harpp, N.; Bao, L. Q.; Black, C. J.; Gleason, J. G.; Smith, R. A. *J. Org. Chem.* **1975**, *65*, 3420.
- Sacripante, G.; Edward, J. T. *Can. J. Chem.* **1982**, *60*, 1982.

(Received 16 June 1994)